Simulation of dilute pneumatic conveying with different types of bends by CFD-DEM

J Du, G M Hu, Z Q Fang, J Wang

School of Power and Mechanical Engineering, Wuhan University, Wuhan 430072, China

E-mail: dujun@whu.edu.cn

Abstract. Bends are one of the most commonly used facilities to change flow direction in pneumatic conveying. It is important to understand the effect of the bend to the gas-solid flow structures in a pneumatic conveying system. CFD-DEM is one of powerful methods to study the fundamentals of gas-solid flow, as it takes the particle-particle and particle-wall collisions into account. But the time consumption is one of major limitations for its application. In this paper, a three-dimensional CFD-DEM model which ignores the effect of void fraction to the gas phase is used to simulate the dilute gas-solid flow. Gas-solid flows in different types of bends including horizontal-vertical, vertical-horizontal and horizontal-horizontal 90 °bends are studied. The present CFD-DEM model is verified by compared the rope structure with the result for traditional CFD-DEM model in horizontal-vertical case. Compared the particle rope dispersion in different types of bends, the rope disperses more quickly in the vertical-horizontal case than others, and the solid flow structure is the most complicated in the horizontal-horizontal case. As their various solid flow structures, the collision data of three cases also seem different.

1. Introduction

Pneumatic conveying is a method of transportation of granular particles in a pipeline using a gas stream. It is widely used in industries because of its cleanness, flexibility of layout, low maintenance cost and a high level of automation. In recent years, with the rapid development of the computer technology, numerical methods have been widely used to research pneumatic conveying. Generally speaking, there are three popular models in modelling gas-solid flow, including Two-Fluid Model (TFM), Direct Numerical Simulation (DNS), and coupled Computational Fluid Dynamics and Discrete Element Method (CFD-DEM) [1]. Previous studies have compared their advantages and disadvantages [2].

In CFD-DEM, the flow of continuum gas phase was determined by Computational Fluid Dynamics (CFD), and the discrete particle phase was obtained by Discrete Element Method (DEM). CFD has been widely accepted in engineering application as its capability to implement complex geometry simulation. Especially with the development of the commercial CFD software package, it continued to expand the scope of application and offered new ways to solve practical engineering problems. DEM is proposed by Cundall and Strack in 1979, which is effective to study particle flow as it accounts for particle-particle and particle-wall interactions. The CFD-DEM has been used by various investigators to study gas-solid flow including pneumatic conveying since it proposed by Tsuji [3, 4, 5, 6].

Bends, which are one of the most commonly used facilities to change flow direction in pneumatic conveying, are known to be one of the key parameters affecting the gas-solid flow structures, such as rope formation, dispersion, and particle segregation [7]. In this work, a three-dimensional CFD-DEM model which is suitable for dilute phase is used to simulate the gas-solid flow in pneumatic conveying pipes with a bend. Compared with the traditional CFD-DEM model, the present model is less compute-intensive, and keeps the simulation effective in dilute phase where the solid volume fraction is low. The simulation is performed by the commercial simulation software EDEM coupled with Fluent. Firstly, the simulation model will be introduced. Subsequently, the result of horizontal-vertical case will be compared with the result for the traditional CFD-DEM model for its verification. Finally, the solid flow structures and collision data for different types of pneumatic conveying systems with a bend will be studied to implement the applications of this model.

2. Mathematical Model

In the present CFD-DEM model, only the mutual momentum exchanges between the gas and solid phase are taken into consideration, and the effect of the particle solid fraction on the gas phase is neglected. In every time step, there is no need to calculate the volume fraction of the gas phase [8].

2.1. Gas phase (CFD)

The continuum gas field uses the existing Navier-Stokes equations in FULENT. In the coupling module, although two phases are created in FLUENT, the conservation equations for solid phase are not solved.

The equation for conservation of mass, or continuity equation, can be written as follows:

$$\frac{\partial \rho_g}{\partial t} + \nabla \cdot \left(\rho_g \boldsymbol{u}_g\right) = 0 \tag{1}$$

The equation for conservation of momentum can be expressed as follows:

$$\frac{\partial}{\partial t}\left(\rho_g \boldsymbol{u}_g\right) + \nabla \cdot \left(\rho_g \boldsymbol{u}_g \boldsymbol{u}_g\right) = -\nabla p + \nabla \cdot \left(\mu_g \nabla \boldsymbol{u}_g\right) + \rho_g \boldsymbol{g} - \boldsymbol{S} \tag{2}$$

Where ρ_g, $\boldsymbol{u}_g$, and $\boldsymbol{g}$ are the gas density, gas velocity and gravity force vector, respectively. μ_g denotes the gas viscosity, and $\boldsymbol{S}$ is the momentum sink. The coupling between the two phases is then achieved through the calculation of the momentum sink of the drag force that arises due to the relatively velocity between the phases. Therefore, the momentum sink $\boldsymbol{S}$ is calculated by

$$\boldsymbol{S} = \frac{1}{\Delta V}\sum_{i=1}^{n} \boldsymbol{f}_{drag,i} \tag{3}$$

Where $\Delta V = \Delta x \Delta y \Delta z$, Δx, Δy and Δz are control volume lengths, $\boldsymbol{f}_{drag,i}$ is fluid drag force which is explained in Section 2.2.

2.2. Solid phase (DEM)

According to DEM, a particle in a system can have two types of motion: translational and rotational, determined by Newton's second law of motion [9]. The forces acting on a particle include gravity, contact force, drag force and other force, such as the van der Waales force and the capillary force. For simplicity, they are not considered in this work. Therefore, the governing equations for particle *i*, at any time, *t*, can be expressed as follows:

$$m_i \frac{d\boldsymbol{v}_i}{dt} = \boldsymbol{f}_{p-g,i} + m_i \boldsymbol{g} + \sum_{j=1}^{k_i}\left(\boldsymbol{f}_{contact,ij} + \boldsymbol{f}_{damp,ij}\right) \tag{4}$$

and

$$\boldsymbol{I}_i \frac{d\boldsymbol{\omega}_i}{dt} = \sum_{j=1}^{k_i} \boldsymbol{T}_{ij} \tag{5}$$

Where m_i, $\boldsymbol{I}_i$, $\boldsymbol{v}_i$, $\boldsymbol{\omega}_i$ and k_i are, respectively, the mass, moment of inertia, translational and rotational velocity, and number of contacting particles of particle i. The forces involved are: the particle-gas interaction force, $\boldsymbol{f}_{p-g,i}$, gravitational force, $m_i \boldsymbol{g}$, and interaction forces between particle i and j, including the contact force, $\boldsymbol{f}_{contact,ij}$, and the viscous contact damping force, $\boldsymbol{f}_{damp,ij}$, Both of which have the normal and tangential components.

The equations used to calculate the forces and torques considered in this work have been listed in table 1, and the coupling scheme is the same as that used in our previous study [10]. As such, it is not given in this paper.

Table 1. The formulation of forces and torques acting in governing equations[a].

Forces and torques	Symbol	Formulation
The normal contact force	$\boldsymbol{f}_{n,ij}$	$(4/3)E^*R^{*1/2}\delta_n^{3/2}$
The normal damping force	$\boldsymbol{f}^d_{n,ij}$	$-2(5/6)^{1/2}\beta(S_n m^*)^{1/2}\boldsymbol{v}_n^{rel}$
The tangential contact force	$\boldsymbol{f}_{t,ij}$	$S_t\delta_t$
The tangential damping force	$\boldsymbol{f}^d_{t,ij}$	$-2(5/6)^{1/2}\beta(S_t m^*)^{1/2}\boldsymbol{v}_t^{rel}$
The torque	$\boldsymbol{T}_i$	$-\mu_t \boldsymbol{f}_n R_i \omega_i$
The drag force	$\boldsymbol{f}_{drag}$	$0.5C_D\rho_g A\lvert\boldsymbol{v}_{p\text{-}g}^{rel}\rvert\boldsymbol{v}_{p\text{-}g}^{rel}$

[a] Where $1/E^*=(1-v_i^2)/E_i+(1-v_j^2)/E_j$, $1/R^*=1/R_i+1/R_j$, $1/m^*=1/m_i+1/m_j$, $\beta=\ln e/(\ln^2 e+\pi^2)^{1/2}$, $S_n=2E^*(R^*\delta_n)^{1/2}$, $S_t=8G^*(R^*\delta_n)^{1/2}$, $1/G^*=(2-v_i)/G_i+(2-v_j)/G_j$, $A=\pi R_i^2$, $Re=\varepsilon_g\rho_g D_p\lvert\boldsymbol{v}_{p\text{-}g}^{rel}\rvert/\eta_g$,

$$C_D=\begin{cases}24/Re & Re\le 0.5\\ 24(1.0+0.15Re^{0.687})/Re & 0.5\le Re\le 1000\\ 0.44 & Re>1000\end{cases}$$

$G_i=E_i/2(1+v_i)$,

3. Simulation Condition

In this work, there are three types of pipe systems simulated: the horizontal-vertical case, the vertical-horizontal case and the horizontal-horizontal case. The geometry of each case consists of three parts: the pipe with the inlet, the 90 ° bend section and the pipe with the outlet. The length of pipe with the inlet and the outlet are 0.5 m and 1 m, respectively. The sketches of the calculation domain of three cases are given in figure 1. The diameter of the pipe D=0.05 m and the bend radius ratio R/D=1.0. The parameters used in three cases are shown in table 2 and table 3.

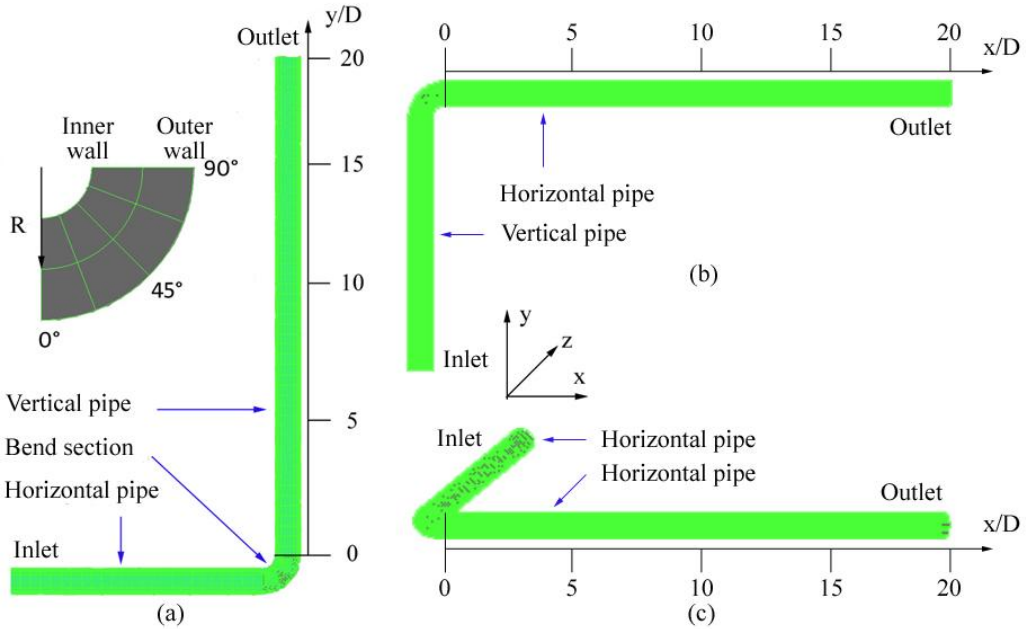

Figure 1. Schematic representation of the simulation: (a) the horizontal-vertical case; (b) the vertical-horizontal case; (c) the horizontal-horizontal case.

Table 2. The same parameters used in three cases.

Phase	Parameter	Symbol	Units	Value
Solid	Density	ρ	kg/m^3	1123
	Poisson ratio	v_i	(-)	0.3
	Shear modulus	G	Pa	1×10^7
	Coefficient of restitution	e	(-)	0.4
	Coefficient of static friction	μ_s	(-)	0.3
	Coefficient of rolling friction	μ_r	(-)	0.005
	Time step		s	1×10^{-6}
	Particle velocity at inlet	$\boldsymbol{v}_i$	m/s	7
Gas	Density	ρ_g	kg/m^3	1.225
	Viscosity	μ_g	kg/m·s	1.8×10^{-5}
	Time step		s	1×10^{-4}

Table 3. The different parameters used in three cases.

				Value		
Phase	Parameter	Symbol	Units	the horizontal-vertical case	the vertical-horizontal case	the horizontal-horizontal case
Solid	Mass flow rate	G_s	kg/m^{2}s	31.1	40.8	35.7
	Particle radius	R_i	mm	1.4	1.5	1.5
Gas	Velocity	$\boldsymbol{u}_g$	m/s	11.9	16	16

4. Results and discussion

For the purpose of model verification, the horizontal-vertical case is calculated first, and compares with the result for traditional CFD-DEM model. The key features of gas-solid flow in a bend including the airflow field, solid flow structure, and particle velocity reduction are obtained by both of the models.

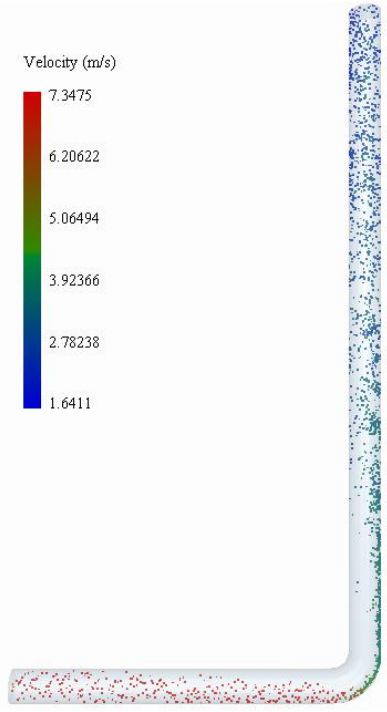

Figure 2. The solid flow structure and the particle velocity of horizontal-vertical case at t=2 s.

The particle rope formation and its dispersion are considered as the most typical characteristic of gas-solid flow in a system with bends and can be captured by the present CFD-DEM model as shown in figure 2. The rope carries most of the conveyed materials in a small portion of the pipe cross-section which locates the outer wall of the bend, and begins to disperse once it moves downstream of the bend in the vertical direction.

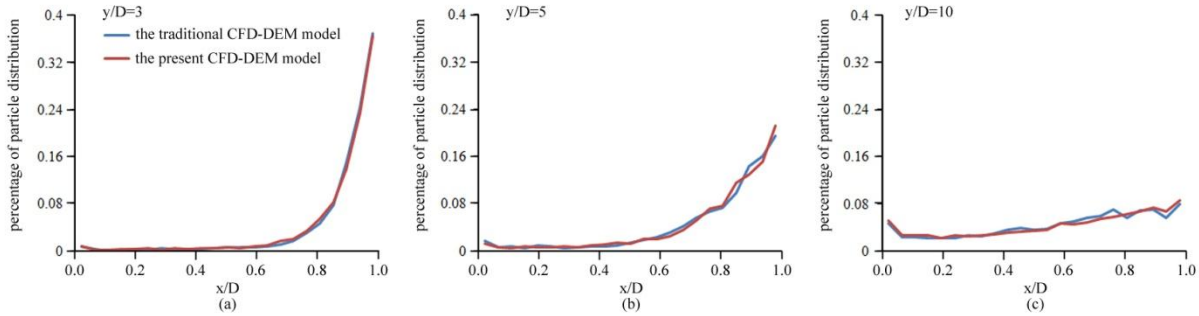

Figure 3. The number of particles at different cross-sections in the vertical pipe from t=1 s to t=3 s: (a) y/D=3, (b) y/D=5, (c) y/D=10.

Figure 3 compares the particle distribution percentage from the inner wall (x/D=0.0) to the outer wall (x/D=1.0) at different locations in the vertical pipe. The particle distributions for the present CFD-DEM model and the traditional CFD-DEM model are remarkably consistent at different locations. It illustrates that the present CFD-DEM model has similar simulation applicability with the traditional one in dilute phase, and can be used to study dilute pneumatic conveying.

Figure 4. The solid flow structure and the particle velocity of vertical-horizontal case at t=2s.

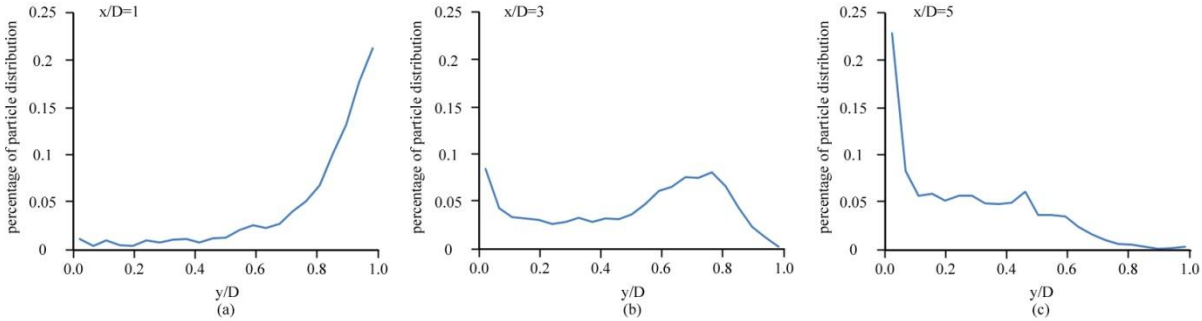

Figure 5. The number of particles at different cross-sections in the horizontal pipe from t=1 s to t=2.5 s: (a) x/D=1, (b) x/D=3, (c) x/D=5.

The solid flow structure of vertical-horizontal case is shown in figure 4. Because of the gravity, the particles deposit at the bottom of the horizontal pipe after the rope dispersion. The percentages of particle distribution from the inner wall (y/D=0.0) to the outer wall (y/D=1.0) at different locations in the horizontal pipe are shown in figure 5. The rope dispersion has completed at x/D=3, and the particles begin to cluster to the bottom at x/D=5. Compared with the rope dispersion in horizontal-vertical case, its dispersion rate is obviously higher.

The solid flow structure of horizontal-horizontal case seems more complicated than the previous cases, as shown in figure 6. The particle rope does not disperse directly to the low particle concentration space, but moves along with a spiral line and keeps close to the inside of the pipe when they exit from the bend section. However, they finally drop to the bottom of the pipe and move to downstream, as the effect of gravity.

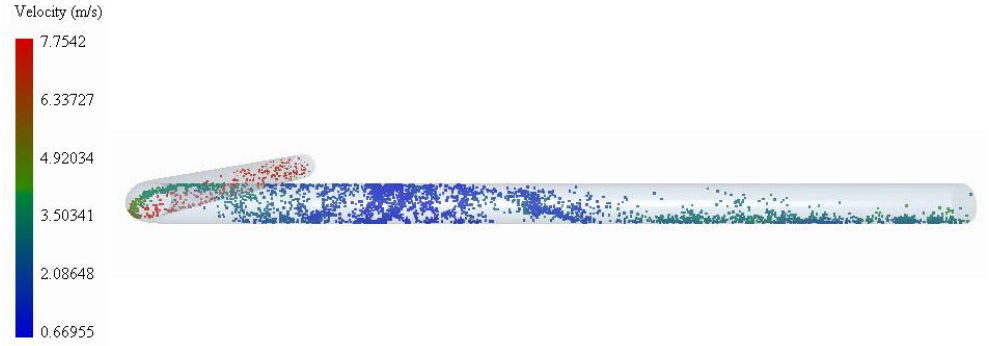

Figure 6. The solid flow structure and the particle velocity of horizontal-horizontal case at t=2s.

Figure 7 shows the particle distribution of the horizontal-horizontal case at the downstream of the bend from t=1 s to t=2.5 s. At exit of the bend (x/D=0), the particle rope is strong, and the particles distribute in a small area. The particles distribute around the whole circum of the pipe at x/D=5, and keep close to the inside of the pipe. Note that the particles distribute the whole circum during t=1 s to t=2.5 s, but they concentrate in a particular area at each moment. It indicates that the rope is weak and unstable, but does not completely disperse. The particles distribution is not a full circum at x/D=10, as the particles are difficult to approach to the top of the pipe because of gravity. The particles gradually deposit at the bottom of the pipe, and the rope almost disperses.

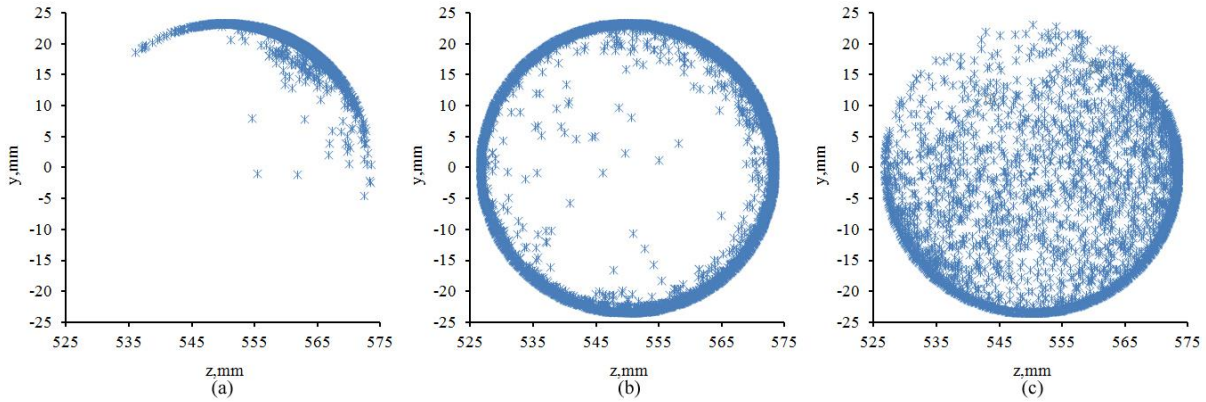

Figure 7. The particle distribution in the horizontal pipe at different locations from t=1s to t=2.5s: (a) x/D=0; (b) x/D=5; (c) x/D=10.

Figure 8 compares the contact data of horizontal-vertical, vertical-horizontal and horizontal-horizontal cases. It indicates that the particle-wall contact is the major contact type at different sections in three cases. The number of contact occurred in bend section is minimum in vertical-horizontal case,

and it relates to the strength of the particle rope formed in the bend. The number of contact which occurred at the downstream of bend section in the horizontal-vertical case is dramatically less than other cases, because the particles finally do not deposit at a particular part, but distribute almost uniformly in the whole pipe.

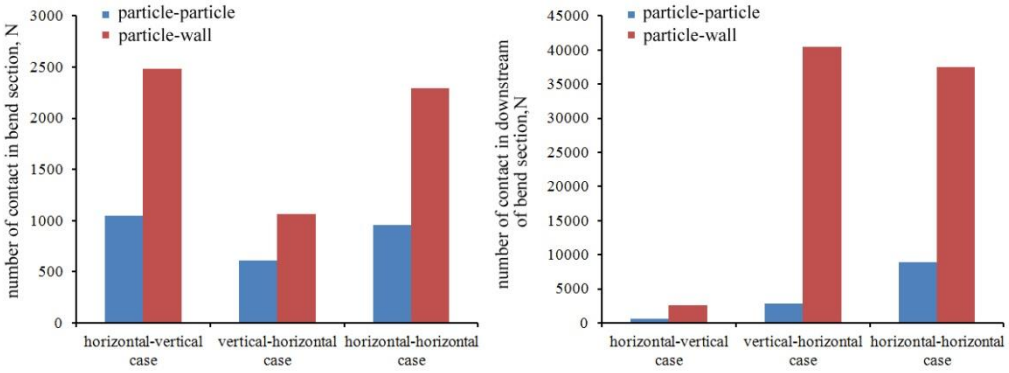

Figure 8. Collision data at different section from t=1s to t=2.5s.

5. Conclusion

The present CFD-DEM model which ignores the effect of the particle solid fraction on the gas phase is used to simulate the gas-solid flow in pneumatic conveying pipes with a bend. Compared the particle rope dispersion rate in horizontal-vertical case, the present CFD-DEM model has a similar result with the traditional CFD-DEM model. It is considered to be suitable for dilute pneumatic conveying simulation. The particle rope formation and dispersion seem different features in horizontal-vertical, vertical-horizontal and horizontal-horizontal cases. The rope dispersion rate of vertical-horizontal case is maximum and the dispersion feature of horizontal-horizontal case seems more complicated. It illustrates that the layout of pipe and bend has significant influence on the solid flow structure and the contact condition.

References

[1] Yu A B and Xu B H 2003 Particle-scale modelling of gas-solid flow in fluidisation *J. Chem Technol Biotechnol.* 78 111-21
[2] Zhu H P, Zhou Z Y, Yang R Y and Yu A B 2007 Discrete particle simulation of particulate systems: Theoretical developments *Chemical Engineering Science.* 62 3378-96
[3] Tsuji Y, Tanaka T and Ishida T 1992 Lagrangian numerical simulation of plug flow of cohesionless particles in a horizontal pipe *Powder Technology.* 71 239-50
[4] Tsuji Y, Kawaguchi and Tanaka T 1993 Discrete particle simulation of two-dimensional fluidized bed *Powder Technology.* 77 79-87
[5] Xu B H and Yu A B 1997 Numerical simulation of the gas-solid flow in a fluidized bed by combining discrete particle method with computational fluid dynamics *Chemical Engineering Science.* 52 2785-809
[6] Zhou Z Y, Kuang S B, Chu K W and Yu A B 2010 Discrete particle simulation of particl-fluid flow: model formulations and their applicability *J. Fluid Mech.* 661 482-510
[7] Chu K W and Yu A B 2008 Numerical simulation of the gas-solid flow in three-dimensional pneumatic conveying bends *Ind. Eng. Chem. Res.* 47 7058-71
[8] Teng S L, Wang P, Zhang Q and Gogos C 2011 Analysis of fluid energy mill by gas-solid two-phase flow simulation *Powder Technology.* 208 684-93
[9] Hu L, Hu G M, Wan H, Liu M Q and Chen J X 2010 Analysis and optimization of operating parameters of ball mills using discrete element method simulation Engineering Journal of Wuhan University. 43 762-9
[10] Du J, Hu G M, Fang Z Q and Fan Z 2014 Simulation of dilute pneumatic conveying with bends by CFD-DEM *Journal of National University of Defency Technology.*